# LANGMUIR

pubs.acs.org/Langmuir Article

# Label-Free Sensitive Detection of Steroid Hormone Cortisol Based on Target-Induced Fluorescence Quenching of Quantum Dots

Ye Liu, Bo Wu, Ekembu K. Tanyi, Sanjida Yeasmin, and Li-Jing Cheng\*



Cite This: Langmuir 2020, 36, 7781-7788



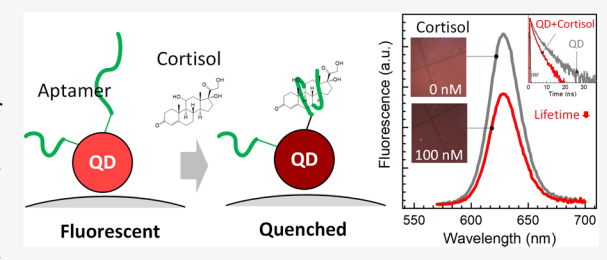
**ACCESS** 

Metrics & More

Article Recommendations

3 Supporting Information

ABSTRACT: We discovered that several types of steroid hormones quench the fluorescence of quantum dots (QDs) at close proximity. Inspired by the finding, we developed a new type of biosensor for the sensitive detection of cortisol via direct fluorescence quenching of functionalized QD probes directly induced by the capture of target cortisol without additional reporter reagents. The detection selectivity was provided by cortisol-selective aptamers or anticortisol antibodies conjugated on the QD surfaces. With the magnetic nanoparticle labeling, the new sensing method enabled rapid cortisol sensing at physiologically



relevant concentrations and yielded the detection limit of  $\sim$ 1 nM for aptamer-based sensors and  $\sim$ 100 pM for antibody-based sensors. We also evaluated the new detection method using saliva samples with an optimized sample preparation process under the assistance of magnetic manipulation. The result showed a satisfying recovery rate for spiked saliva tests. The facile sensing technology offers an appealing approach for the detection of steroid hormones in point-of-care settings.

# **■ INTRODUCTION**

Cortisol is released into the body during stressed and agitated status. It is considered as a biomarker for many diseases such as Cushing's syndrome, chronic fatigue syndrome, post-traumatic stress disorders, and fibromyalgia, which are results of excesses or deficiencies of cortisol. Quantitative analysis of hormone cortisol has been widely adopted for the management of psychological stress and diagnosis of chronic diseases related to cortisol disorders. 1-3 Cortisol concentrations in the body fluctuate throughout the day and night in a circadian rhythm with levels being the highest in the morning (5 nM—hundreds of nanomolar) and the lowest in the evening or at midnight (<2 nM). Measurements of late-night salivary cortisol and 24 h urine cortisol are among the first-line screening tests for Cushing's syndrome.<sup>4</sup> The cutoff values of late-night salivary cortisol for the diagnosis of Cushing's syndrome may differ among different testing laboratories. A wide range of diagnostic cutoff levels from 4 (145 ng/dL) to 15.2 nM (550 ng/dL) has been reported in the previous studies.4-6

Cortisol levels are conventionally measured through antibody-based enzyme-linked immunosorbent assay (ELISA),<sup>7–9</sup> which offers high affinity and specificity to targets. <sup>10</sup> However, ELISA typically requires additional labeling of chromogenic reporters to produce observable colorimetric or fluorescence readout. The immunosensor also has a short shelf-life; long-term storage may deteriorate the performance of detection. <sup>11</sup> Apart from antibody-based assays, cortisol-selective aptamers have been demonstrated for cortisol detection accompanied by additional labeling for electrochemical or optical sensing readouts. <sup>2,12,13</sup> Nucleic acid aptamers are relatively stable at room temperature and are accessible for various ionic buffers,

making them suitable for the applications in point-of-care diagnostics.  $^{14-20}$ 

A variety of biosensors have been reported for sensitive salivary cortisol detection, such as surface plasmon resonance-based sensors, <sup>21,22</sup> electrochemical sensors, <sup>23,24</sup> and colorimetric sensors based on molecularly imprinted polymer. <sup>25</sup> Here, we present a nanoparticle-based cortisol sensor that utilizes magnetic manipulation to simplify sample preparation and detection processes. Besides, the nanosensor offers a fast sensing response in a solution by taking advantage of the rapid three-dimensional diffusion of target molecules. <sup>26</sup> The diffusion of targets toward the sensor surface is further expedited as the size of sensor particles is reduced to the nanometer scale. <sup>26</sup>

We observed fluorescence quenching of quantum dots (QDs) induced by multiple types of steroid hormones and confirmed the results through fluorescence lifetime measurements. The phenomenon enlightened us to develop QD-based cortisol nanosensors that analyze the cortisol concentration by measuring the direct quenching of fluorescence intensity without additional labeling. QDs have advantages over traditional organic fluorophores in strong and stable fluorescence emission with the color adjustable by the

Received: February 23, 2020 Revised: June 16, 2020 Published: June 17, 2020





size.<sup>27,28</sup> Also, the surface of each QD contains numerous functional groups available for the conjugation of multiple probes. The configuration can hardly be attained using organic fluorophores. The selectivity of the cortisol detection was achieved by either the anticortisol antibodies or cortisol-selective aptamers tethered on CdSe/ZnS core—shell QDs. The aptamer-conjugated or antibody-conjugated QDs were carried by ~20 nm-sized magnetic nanoparticles (MNPs) to form aptamers—QD@MNP or antibody—QD@MNP nanosensors, as illustrated in Figure 1a. The MNP carriers facilitate

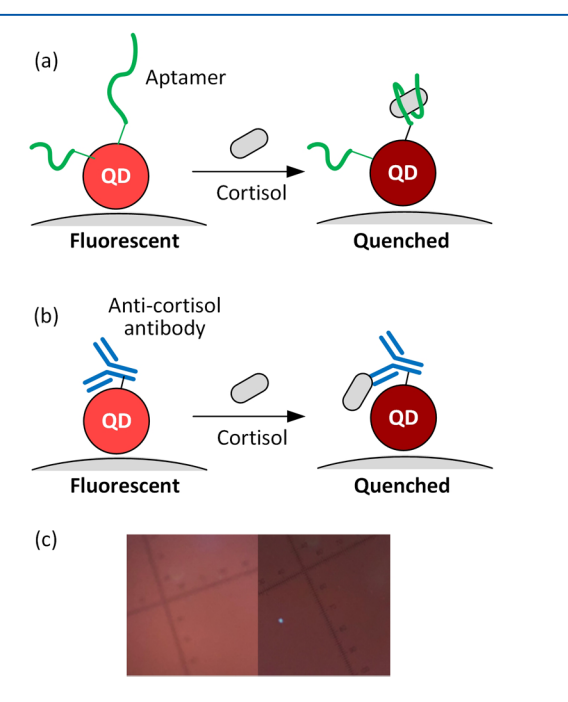


Figure 1. Schematics of cortisol detection using target-induced quenching based on (a) aptamer-conjugated QDs and (b) antibody-conjugated QDs carried by a magnetic nanoparticle (MNP). The detection relies on the quenching efficiency modulated by the number of the captured cortisol on each QD. (c) Fluorescence images of aptamer-based nanosensors in the analyte solutions in the absence of cortisol (left) and the presence of 100 nM target cortisol (right).

probe conjugation, sample preparation, and cortisol detection in saliva samples. Both types of cortisol nanosensors exhibit a decrease in fluorescence intensity in response to the capture of cortisol. The number of captured cortisol modulates the quenching efficiency of the QDs. The simple detection approach enabled rapid cortisol sensing at physiologically relevant concentrations (<1 nM to hundreds of nanomolar) and yielded a detection limit of about 1 nM for the aptamerbased nanosensors and 100 pM for the antibody-based nanosensors. The sensing approach can be extended to detect other steroid hormones that exhibit similar capability of fluorescence quenching. We further demonstrated the sensitive detection of cortisol in saliva under the assistance of magnetic manipulations for sample preparation. The results indicate the potential of using target-induced fluorescence quenching assay for the point-of-care diagnosis that relies on the analysis of steroid hormones.

# **■ EXPERIMENTAL SECTION**

**Material and Chemicals.** Carboxyl-functionalized CdSe/ZnS QDs with 540 and 630 nm emission wavelengths were purchased from Cytodiagnostics, LLC (Ontario, Canada). Carboxyl-function-

alized 540 nm CdSe/ZnS QDs with 4 nm polymer coating were obtained from Ocean NanoTech, LLC (San Diego, CA). 1-Ethyl-3-(3-dimethylaminopropyl)carbodiimide hydrochloride (EDC), Nhydroxysulfosuccinimide (sulfo-NHS), 10× phosphate-buffered saline (PBS) buffer, and 2-(N-morpholino)ethanesulfonic acid (MES) were obtained from Thermo Fisher Scientific (Waltham, MA). N-(2-Aminoethyl)maleimide trifluoroacetate salt, monopotassium phosphate (KH<sub>2</sub>PO<sub>4</sub>), [3-(2-aminoethylamino)propyl]trimethoxysilane (AEAPTMS), N-succinimidyl N-methylcarbamate, and steroid hormones, including hydrocortisone (cortisol),  $\beta$ -estradiol, estriol, estrone, and progesterone, were obtained from Sigma-Aldrich (St. Louis, MO). Dehydroepiandrosterone (DHEA) was obtained from Chem-Impex International (Wood Dale, IL). Cortisone was obtained from Alfa Aesar (Haverhill, MA). The nucleic acid aptamer probe against cortisol is a 3'-amino-modified oligonucleotide with a sequence of 5'-GGAAT GGATC CACAT CCATG GATGG GCAAT GCGGG GTGGA GAATG GTTGC CGCAC TTCGG CTTCA CTGCA GACTT GACGA AGCTT-3' obtained from LGC Biosearch Technologies (Novato, CA). Anticortisol mouse monoclonal antibody (XM210) was purchased from Novus Biologicals (Littleton, CO). A saliva sample was obtained from Pickering Laboratories (Mountain View, CA). Sylgard 184 silicone elastomer (poly(dimethylsiloxane)—PDMS) was obtained from Dow (Midland,

Steroid Hormone-Induced Fluorescence Quenching of QD-Coated Glasses. Amine-functionalized glasses were produced by incubating the glass slides in a silane solution containing 1% AEAPTMS, 5% acetic acid methanol solution. QDs were immobilized on the glass through a typical amine-reactive reaction using 50 nM carboxylated QDs, 2 mM EDC, and 5 mM sulfo-NHS in dimethylformamide (DMF) for 4 h. After rinsing and drying, we introduced multiple types of steroid hormones of various concentrations in an ethanol—water solution (1:1 in volume) to the QD-coated glass substrates enclosed by PDMS microfluidic channels for fluorescence measurement. Fluorescence images were captured after 1 min incubation of the analyte solution.

Synthesis of Aptamer/Antibody-Conjugated QD Probes Carried by MNPs (Aptamer–QD@MNP and Antibody–QD@MNP). Amine-functionalized magnetic nanoparticles (MNPs) were synthesized based on the method reported in the previous work. Carboxylated QDs were immobilized on the amine-functionalized MNPs using a typical EDC–NHS coupling reaction. A 100  $\mu$ L of mixture of 50 nM carboxylated QDs, 2 mM EDC, and 5 mM sulfo-NHS in DMF was first incubated for 15 min and mixed with an 8  $\mu$ L amine-functionalized MNP solution (0.16 mg/mL) in DMF to react for 1.5 h. Finally, the unreacted amine groups on the MNPs were quenched by reacting with 10 mM N-succinimidyl N-methylcarbamate in 1× PBS buffer.

Aptamers were conjugated on the QD@MNP nanosensors by mixing the 37.5 nM NHS-activated QDs on MNP with 8 µM aminefunctionalized aptamer oligonucleotide probes in 2× PBS buffer for 12 h. The molar ratio of DNA to QDs was controlled to be 8:0.05, sufficient to minimize the nonconjugated QDs. The product was rinsed and redispersed in 0.1× PBS buffer, which may then be stored at 4 °C until ready for assay. Absorbance measurements based on Nanodrop 2000c were performed to analyze the change in aptamer concentration in the supernatant of the reaction mixture before and after the conjugation process. The result suggests that about four aptamers were attached to each QD through the conjugation processes. We found that an aptamer concentration greater than 6 µM was required to achieve the consistent result. The antibody-QD@MNP complexes were produced by a similar approach except that the probe conjugation was carried out using 0.05 mg/mL anticortisol antibodies in 1× PBS buffer for 45 min, followed by multiple rinsing with standard PBS buffer. Each QD was estimated to contain at least two antibody molecules based on the same absorbance measurement.

**Cortisol Detection Assay.** The assay was carried out by mixing 150  $\mu$ L of analyte of various target cortisol concentrations ranging from 100 pM to 100 nM in 0.1× PBS buffer with 50  $\mu$ L, 10 nM

aptamer–QD@MNP solution or antibody–QD@MNP for 20 min. This assay was repeated to evaluate detection selectivity in the presence of multiple types of steroid hormones, including DHEA, cortisone,  $\beta$ -estradiol, estriol, estrone, and progesterone. The sensing performance was characterized by measuring fluorescence spectra in a 500  $\mu$ L cuvette using a spectrofluorometer.

Optical Characterization. The fluorescence spectra of aptamer-QD@MNP and antibody-QD@MNP nanosensors were measured in a solution to characterize cortisol detection using a spectrofluorometer (FluoroMax-4c, Horiba) with 380 nm wavelength excitation. Steroid hormone-induced QD fluorescence quenching was performed on a glass substrate and analyzed using an inverted fluorescence microscope (Olympus IX73) through a 40× objective lens under UV excitation with a spectral range from 350 to 400 nm produced by a light-emitting diode (LED) excitation (X-Cite 120) and a filter set (DAPI-50LP). The fluorescence signals were characterized by a monochromic sCMOS camera (Hamamatsu Flash 4.0 LT) on the microscope. The color fluorescent images were captured by a color charge-coupled device (CCD) camera (Lumenera Infinity3-3UR). The fluorescent images were taken with background subtraction, and the same setting was used throughout the experiment. Fluorescence lifetime measurements were accomplished using a time-correlated single-photon counting (TCSPC) system (Picoharp 300, PicoQuant) and 375 nm UV pulsed laser excitation.

Cortisol Detection in Spiked Saliva Samples. The cortisol spiked saliva sample was first diluted five times with PBS buffer. We incubated 10  $\mu$ L of a nanosensor solution with the 190  $\mu$ L of a diluted cortisol spiked saliva sample for 20 min. The mixture was then washed at least three times using 2× PBS rinsing buffer under external magnetic fields to remove the saliva completely. After the final washing step, the nanosensor mixture was dispersed in 50  $\mu$ L 2× PBS buffer. The mixture was then diluted four times with deionized water, resulting in a nanosensor solution in 0.5× PBS buffer for fluorescence detection.

#### RESULTS AND DISCUSSION

Fluorescence Quenching of QDs Induced by Steroid Hormones. We observed different levels of QD fluorescence quenching caused by eight types of steroid hormones, including cortisol, cortisone, DHEA, estrone, progesterone, estriol, and  $\beta$ -estradiol, with the chemical structures shown in Figure 2a. The steroid hormone-induced fluorescence quenching was analyzed individually in separate PDMS fluidic wells sealed on top of a 540 nm QD-coated glass substrate, as illustrated in Figure 2b. We introduced three different concentrations of steroid hormones (1  $\mu$ M, 100  $\mu$ M, and 10 mM) in an ethanol-water solution (1:1 in volume) for qualitative analysis. These concentrations were chosen to arrange enough free steroid hormone molecules nearby the QDs on the glass surface, resembling the concentration of steroid hormones captured by the QD nanosensors that contain receptors. Because of the high concentration of steroid hormones employed for the tests, the ethanol-water solution (1:1 in volume) was used as the solvent to promote solubility. The steroid hormone solutions of such concentration range did not yield any distinguishable change in optical absorption over the range of the fluorescence excitation and emission wavelengths. Figure 2c lists the fluorescence images of the QDcoated glass at the boundaries of the PDMS fluidic wells filled with different steroid hormones of various concentrations in the ethanol-water solution (1:1 in volume). The right half of each image is the well area with the QD-coated glass exposed to a steroid hormone solution of concentrations C, providing the fluorescence intensity measured to be  $I_{\rm C}$ . The left half of the image has the QD-coated surface sealed under PDMS that gives a reference fluorescence intensity  $I_{Ref,C}$  corresponding to

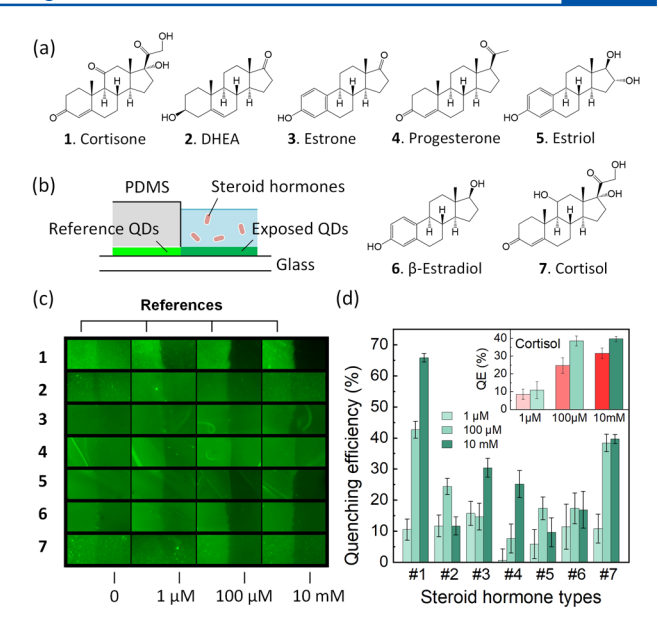


Figure 2. (a) Chemical structures of the steroid hormones under test. (b) Schematic of the fluidic well setup for testing steroid hormone-induced fluorescence quenching. QDs were immobilized to the glass substrate enclosed by PDMS fluidic wells. (c) Fluorescence images of QD-coated glass substrates exposed to different steroid hormones at various concentrations in the ethanol—water solution (1:1 in volume), including 0, 1  $\mu$ M, 10  $\mu$ M, and 10 mM. (d) Quenching efficiency of immobilized QDs in the presence of different steroid hormone solutions at various concentrations. The inset compares the quenching efficiency (QE) of green QDs (540 nm emission) (green bars) and red QDs (630 nm emission) (red bars) under different cortisol concentrations (n=3).

each specific  $I_{\rm C}$ . As the QDs were covalently immobilized on the glass surface, we did not observe any fluorescence decay due to the detachment of QDs after multiple fluidic manipulations. Figure 2d summarizes the concentration-dependent quenching efficiency induced by different steroid hormones. The quenching efficiency is defined by QE =  $1-I/I_{\rm B}$ , where  $I=I_{\rm C}/I_{\rm Ref,C}$  and  $I_{\rm B}=I_{\rm 0}/I_{\rm Ref,0}$  are the normalized fluorescence intensities for a steroid hormone solution of concentration C and the solution without steroid hormone, respectively.

All of the steroid hormones cause varying degrees of QD fluorescence quenching. Among them, cortisone, progesterone, and cortisol yield the most observable change in fluorescence intensity. Cortisone was observed to quench QDs most efficiently, up to a maximum of 75% at 100 mM. The QD quenching efficiency induced by cortisol increases from 10 to 30% as the cortisol concentration rises from 1  $\mu$ M to 10 mM. Increasing the concentration of DHEA, estriol,  $\beta$ -estradiol, and cortisol solutions to 10 mM does not result in further fluorescence quenching. The reduced or retarded quenching efficiency for some samples may stem from the fact that these steroid hormones have limited solubility and tend to precipitate at millimolar concentrations. The undissolved steroid hormone chunks cannot contribute to fluorescence quenching.

The concentration-dependent fluorescence quenching is associated with not only the number of steroid hormones around each QD but also their distance from the QD. As the molecule concentration increases from 1  $\mu$ M to 10 mM, the intermolecular distances are estimated to reduce from 120 to

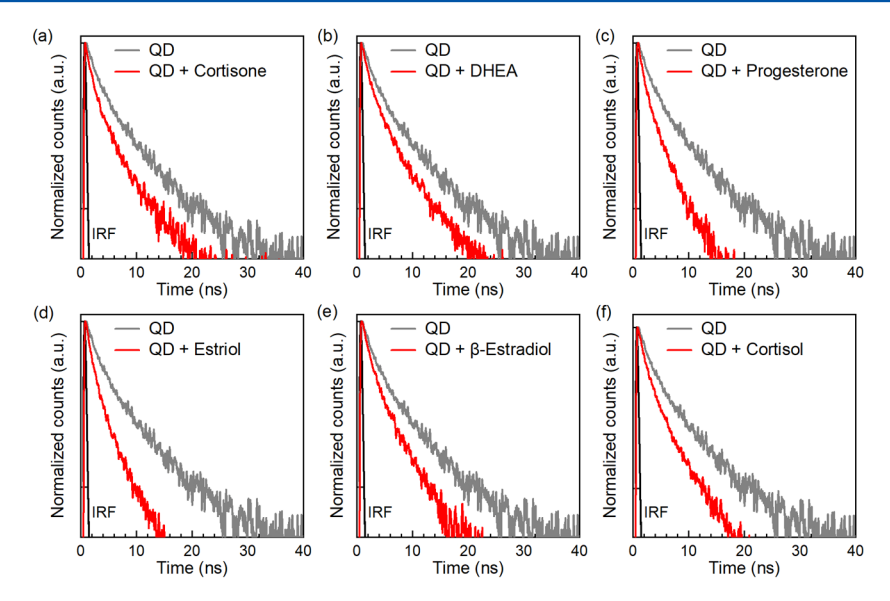


Figure 3. Fluorescence lifetime decays of immobilized QDs in the presence and absence of different 10 mM steroid hormones in the ethanol—water solution (1:1 in volume). The steroid hormones include (a) cortisone, (b) DHEA, (c) progesterone, (d) estriol, (e)  $\beta$ -estradiol, and (f) cortisol.

5.5 nm, and the molecules tend to be located more closely to QDs, leading to a more substantial fluorescence quenching. To verify the effect of molecule-QD distance on quenching efficiency, we repeat the tests using polymer-coated QDs, which contain 4 nm thick polymer shells to separate steroid hormones from QDs further. We observed a negligible change in fluorescence intensity with the increase of the cortisol concentration (Figure S1). It is worth noting that steroid hormones are more soluble in the ethanol-water solution compared to aqueous PBS buffer. Due to the high solubility in the ethanol-water solution, steroid hormones are more likely to stay in the ethanol-water solution rather than accumulate on the QD surface to result in fluorescence quenching. Quenching of green QDs aside, steroid hormones were also found to quench red QDs with 630 nm emission. As shown in the inset of Figure 2d, the quenching efficiency of red QDs reaches about 30% at 10 mM cortisol concentration. The result implies that the steroid hormone-induced QD quenching is likely to be distance-dependent. The regulation of QD fluorescence intensity by cortisol molecules offers the possibility to detect cortisol directly without any labeling. Based on our knowledge, the QDs quenched by steroid hormone have not been reported.

To investigate the fluorescence quenching phenomena, we measured the fluorescence lifetimes of QDs immobilized on glass surfaces in the absence and presence of different steroid hormones in the ethanol-water (1:1) solution. Figure 3 shows the average fluorescence lifetime of the immobilized QDs is 3.3 ns in the steroid hormone-free solution. When the QDs exposed to all different types of steroid hormones, the lifetime reduces to 2.4 (cortisone), 2.6 (DHEA), 2.2 (progesterone), 2.1 (estriol), 2.5 ( $\beta$ -estradiol), and 2.5 ns (cortisol). The fluorescence quenching could be associated with the charge transfer between excited QDs and steroid hormones.<sup>29</sup> These steroid hormones have been found to participate in charge-transfer interactions with fluorophores due to their electron-acceptor capacity of carbonyl groups and the presence of the lpha and eta-unsaturated ketone. Some steroid hormones, such as  $\beta$ -estradiol, exhibit strong electron donor property resulting from the aromatic structure.3

Nanosensors for Cortisol Detection. The cortisol nanosensors were realized by conjugating cortisol receptors on the QDs, which were carried by magnetic nanoparticles, i.e., QD@MNP. The cortisol receptors can be cortisol-selective DNA aptamers or anticortisol antibodies. Each QD may contain multiple cortisol receptors, allowing the capture of numerous target cortisols for efficient fluorescence quenching. We observed fluorescence quenching of QDs upon the conjugation processes. Attachment of QD on MNP quenched the fluorescence intensity of QD by 10%. Immobilization of aptamers on QDs caused a total decrease of 31% in fluorescence intensity compared to the same amount of bare QDs. On the other hand, the QD fluorescence dropped as high as 70% in total after conjugation of antibodies. The severe fluorescence quenching may result from the amino acids on the antibody molecules.3

The quenching efficiency tests shown in the previous section suggest that cortisol quenches green QDs more efficiently than red QDs. However, the aptamer-conjugated QDs revealed an opposite trend. The nanosensors composed of aptamerconjugated red QDs (630 nm emission) yielded a greater intensity change than the aptamer-conjugated 540 nm green QDs in response to the presence of cortisol molecules (Figure S2a). The result could be associated with the fact that the red QDs are larger than the green QDs and provide more surface area for the conjugation of aptamers. More cortisol can be captured on each red QD leading to the greater fluorescence quenching. The result led us to employ red QDs for the cortisol sensors. The ionic strength of the analyte solution was found to affect the sensitivity of the aptamer-based cortisol nanosensors. Figure S2b summarized the effect of the PBS buffer concentration on the quenching efficiency of the aptamer-conjugated QDs in response to 10 nM cortisol. We observed an optimal fluorescence intensity of the QDs and sensitivity of cortisol detection with the PBS concentration between 0.1× and 0.5×. No considerable difference in fluorescence quenching efficiency was observed between the measurements conducted using 0.5× PBS and 0.1× PBS. The condition was chosen for the rest of the assays. The ionic strength has been reported to affect the configuration of DNA aptamer and, therefore, the binding of target molecules to aptamers.<sup>33,34</sup> Strong ionic shielding effect at high ionic strength causes the conformational changes of the aptamer binding site resulting in a lower affinity to its target. At low ionic strength, the increased repulsive electrostatic force within the negatively charged DNA aptamer backbones increases the persistence length and hinders the binding of the target molecules.

**Cortisol Detection Assay.** Figure 4a,b is the fluorescence spectra of the analyte solutions containing aptamer—QD@

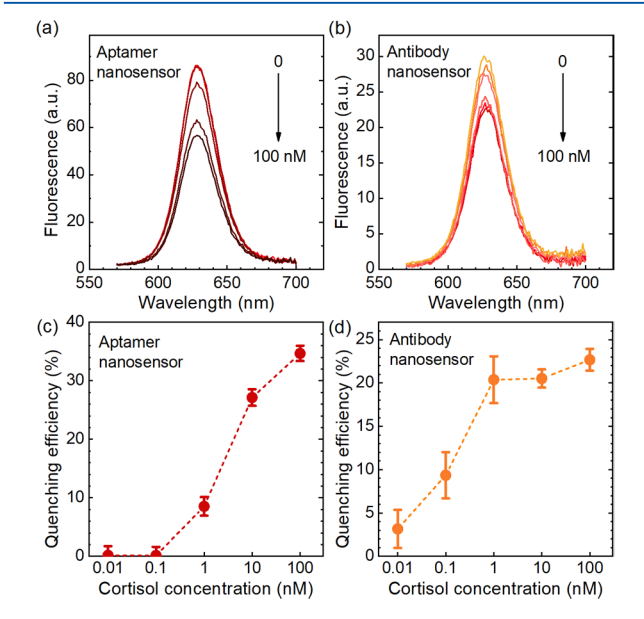


**Figure 4.** Fluorescence spectra of (a) aptamer-based nanosensors (aptamer-QD@MNP) and (b) antibody-based nanosensors (antibody-QD@MNP) in response to cortisol concentrations, ranging from 10 pM to 100 nM in  $0.1 \times$  PBS buffer. Quenching efficiencies of the (c) aptamer-based nanosensors and (d) antibody-based nanosensors at various cortisol concentrations (n = 3).

MNP probes and antibody-QD@MNP probes, respectively, after 30 min incubation with target cortisol of various concentrations. Real-time sensing result in Figure S3 suggests that a 20 min incubation time is sufficient for the capture of target molecules and yields an observable fluorescence quenching for different target concentrations. The fluorescence intensity of the nanosensor-analyte mixture increases dramatically during the first 20 min incubation and saturates after 40 min. The fluorescence intensity decreases by more than 30% for the aptamer-based nanosensors as the target cortisol concentration rises from 10 pM to 100 nM. Figure 4c,d summarizes the quenching efficiencies of the aptamerbased nanosensors and antibody-based nanosensors in response to different cortisol concentrations. A maximum of 35% signal decrease was detected in a 100 nM cortisol analyte solution using aptamer-based nanosensors. The detection limit, defined as three times the standard deviation of the signal measured from the sample without target cortisol, was measured to be about 1 nM. Similarly, the antibody-based nanosensors also exhibit fluorescence quenching in the presence of target cortisol, as shown in Figure 4b,d. However, their fluorescence intensity and quenching efficiency over the same cortisol concentration range were lower compared with aptamer-based nanosensors. The analyte with 100 nM target cortisol contributes 20% quenching efficiency. Figure 4d shows

that the response of antibody-based nanosensors saturates when the cortisol concentration exceeds 10 nM. The lower quenching efficiency of the antibody-based nanosensor could be attributed to the larger size of the antibody molecule that keeps the captured cortisol distant from the QD surface and therefore weakens the efficiency of energy transfer required for fluorescence quenching. The sizes of the cortisol antibody molecule and cortisol aptamer have been reported to be about 9 and 1.5 nm, respectively, measured using atomic force microscopy.<sup>22</sup> Also, the hydrodynamic radius of an 85-base single-stranded DNA aptamer is estimated to be about 2.6 nm at 100 mM ionic strength. See the Supporting Information for calculation details. Note that although the antibody is at about 9 nm high, not all the conjugated antibodies can stand straight out of the QD surface. Since the antibodies are immobilized through their free amine groups appearing at multiple positions in the backbone, the immobilized antibodies are randomly oriented and tend to lay on the surface.<sup>35</sup> Therefore, some of the captured cortisols can stay close to the surface of QDs, resulting in fluorescence quenching. Nevertheless, overall, the quenching efficiency is weaker than the aptamer-based sensors. The measured and theoretical dimensions of the probes imply that the formation of an aptamer-cortisol complex is likely to bring cortisol even closer to the QD surface as opposed to an antibody-cortisol complex, leading to a stronger fluorescence quenching. Aside from the different quenching efficiency, the antibody-based nanosensor also yielded a detection limit of about 100 pM, lower than the 1 nM offered by the aptamerbased nanosensor (Figure 4d). We believe that the difference in the detection limit stems from the high dissociation constant of the aptamer-cortisol complexes.13

**Selectivity.** Figure 5a,b summarizes the detection selectivity of the aptamer-based and antibody-based cortisol nano-

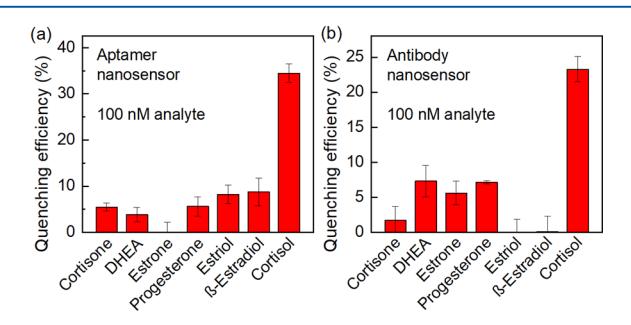


**Figure 5.** Quenching efficiency of the (a) aptamer nanosensor and (b) antibody nanosensor in response to different steroid hormones of 100 nM in  $0.1 \times PBS$  buffer without optimized rinsing steps (n = 3).

sensors, respectively, against different steroid hormones. All of the tests were performed using high-concentration 100 nM steroid analytes in 0.1× PBS with 20 min incubation. The results indicate that cortisol provided the strongest fluorescence quenching of nanosensors compared with the others indicating a good selectivity. Since no rinsing step was applied to these selectivity tests, a small amount of steroid hormone analogs may be still able to nonspecifically attach to the nanosensors, resulting in weak fluorescence quenching. The selectivity can be further improved by applying an optimized rinsing step, which will be discussed in the next section. The selectivity of detection can be contributed by two factors: (1) the selective affinity of the cortisol-selective aptamer and the anticortisol antibody to the target cortisol, and (2) the intrinsic

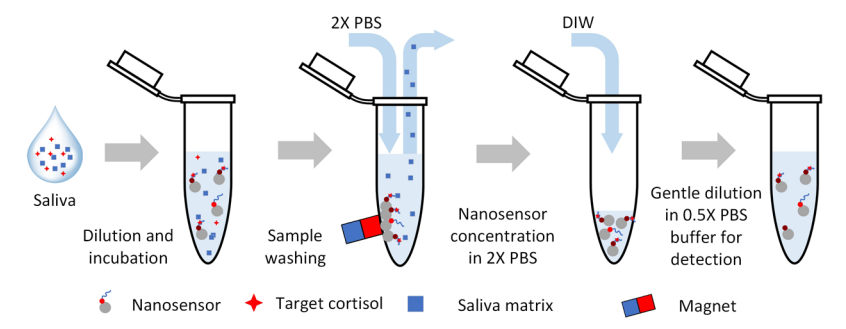
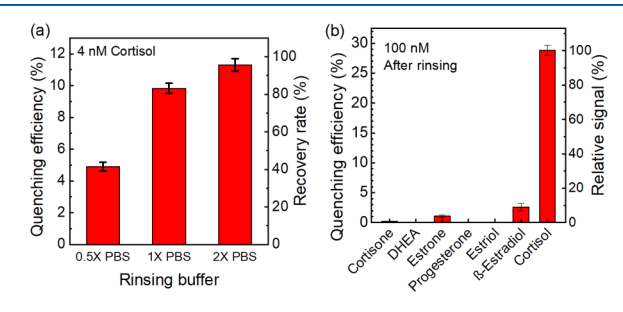


Figure 6. Schematic of sample preparation and detection for cortisol sensing in saliva.

quenching ability of the steroid hormone molecules. The steroid hormones with poor quenching ability will not be detected even they happen to be captured by the nanosensors. The selectivity of the probes was also verified by comparing the quenching efficiency of the nonconjugated bare QD@MNP dispersed in PBS buffer upon the interactions with different steroid hormones. Figure S4 shows that without rinsing, the fluorescence quenching of QD is likely to occur due to the nonspecific binding of steroid hormones on the bare QD surface. The presence of 100 nM steroid hormones, especially cortisone and estriol, not only increased the quenching efficiency of the QD@MNP nanoparticles but also altered the dispersion behavior of the nanoparticles in PBS buffer. Slight aggregation of QD@MNP nanoparticles occurred under the introduction of some steroid hormones. For most of the steroid hormones except estriol, the quenching efficiency was significantly suppressed after a rinsing step. The strong nonspecific binding of estriol may result from its weak solubility in PBS buffer. It is worthwhile to know that due to the lower solubility of steroid hormones in aqueous solutions, the nonspecific binding of steroid hormones on bare QDs is more observable in PBS buffer solutions than in organic solvents, such as the ethanol-water solution presented in Figure 2. The low solubility of steroid hormones in PBS buffer may promote their adsorption to the bare QD surface, which induces stronger fluorescence quenching and assists the aggregation of QD nanoparticle composites leading to further fluorescence quenching. As a result, some steroid hormones, such as cortisone, were found to substantially quench the fluorescence of QD@MNP nanoparticles even at a lower concentration compared with the results shown in Figure 2. The strong quenching due to the nonspecific binding of steroid hormones was significantly reduced with the probe conjugated QD@MNP nanoparticles, which were highly dispersible in PBS buffer even under the exposure of the same concentration of steroid hormones. The improved detection selectivity could result from the steric repulsion between the nontarget steroid hormones and the aptamers or antibody receptors on QDs. We will demonstrate in the next section that an adequately controlled rinsing step can further raise the selectivity of the detection.

Cortisol Detection Using Saliva Samples. The matrix of saliva could negatively impact the interactions between the nanosensors and target molecules. The magnetic property of the nanosensor facilitates the sample preparation of saliva samples for cortisol detection. We illustrate the sample preparation method in Figure 6. The ionic strength of the rinsing buffer was found to affect the final sensing performance significantly. The increase in the ionic strength of the PBS rinsing buffer enhanced the fluorescence quenching efficiency

in response to cortisol binding. As shown in Figure 7a, the final detection recovery rate raises from 42 to 96% as the PBS



**Figure 7.** Effect of rinsing buffer concentration on the quenching efficiencies of the aptamer—QD@MNP probes in the presence of 4 nM cortisol and the recovery rates of the detection (n = 3). (b) Aptamer nanosensor signals in response to different steroid hormones of 100 nM concentration after optimized sample preparation and rinsing process (n = 3).

concentration for sample washing increases from 0.5× to 2×. The result may be attributed to the fact that the buffer ionic strength alters the dynamic morphology of aptamer and, therefore, the cortisol binding affinity. The last dilution step was gently applied without magnetic attraction to obtain a mixture in 0.5× PBS for fluorescence detection. The resulting low ionic strength background was introduced to the sample to improve fluorescence intensity. The final dilution process was performed without magnetic attraction to minimize the flowinduced shear stress that may negatively affect the molecular binding and hence the detection result. We believe that the bound cortisol may dissociate from the aptamer during the sample washing step by cause of the low ionic strength buffer and shear force produced by magnetic manipulation. We chose 2× PBS buffer for sample washing in the rest of the detection assays to assure the binding of captured targets. Figure 7b compares the quenching efficiency of the cortisol aptamer nanosensors in response to different steroid hormones. The detection was conducted using the optimized sample preparation procedure that applied 2× PBS in the rinsing step. Negligible fluorescence quenching of the nanosensors was measured in the presence of nontarget steroid hormones, indicating a high specificity of sensing after the rinsing step.

Dilution of saliva samples was also found necessary for sensitive, robust cortisol detection. The viscous saliva sample suppressed the efficiency of magnetic manipulation, leading to inconsistent sample preparation and detection results. The effect of saliva sample dilution on the detection result is summarized in Figure S5 in the Supporting Information. Our study suggests that fivefold dilution of a saliva sample is

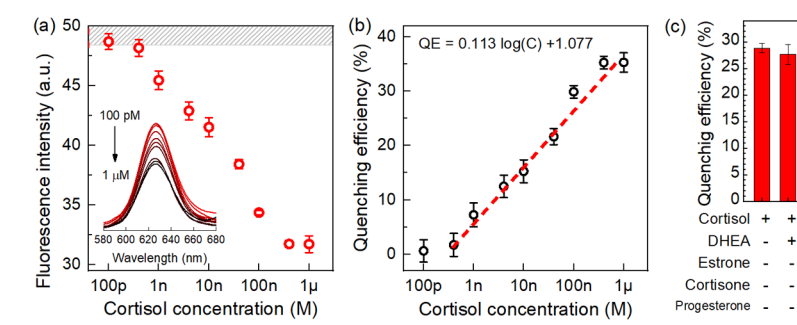


Figure 8. (a) Fluorescence intensity of aptamer—QD@MNP probes in response to various cortisol concentrations in  $0.5 \times PBS$  (n = 3). The inset shows the representative fluorescence spectra of the nanosensor at different cortisol concentrations. (b) Calibration curve of quenching efficiency at various cortisol concentrations. The dashed line represents the linear calibration fit. The samples for calibration went through the sample preparation process. (c) Selectivity test at different combinations of target cortisol, DHEA, estrone, cortisone, and progesterone. The concentrations of all the steroid hormone samples were 100 nM. The error bars represent the standard deviation of the measurements.

practical to achieve the detection results close to those analyzed using 0.5× PBS buffer.

Cortisol solution in 0.5× PBS buffer was used as a calibration standard to evaluate the detection performance. The samples for calibration went through the optimized sample preparation procedure. Figure 8a,b shows the fluorescence intensity and the corresponding quenching efficiency of the nanosensor solution in response to the cortisol concentration. The method yields a limit of detection of <1 nM with the linear quantification range from 0.4 to 400 nM. Figure 8c summarizes the results of cortisol detection in the presence of 100 nM nontarget interferents. The mixtures that contain target cortisol consistently yield strong quenching efficiency. The result proves that the nanosensor can discriminate target with negligible interference from other steroid hormone analogs. The detection of cortisol concentration (C) can be calculated by a linear fit of the quenching efficiency (QE) =  $0.113 \log(C) + 1.077 \text{ with } R^2 = 0.984.$  To validate the clinically relevant assay, we spiked 12.5 and 125 nM cortisol in saliva samples and conducted fivefold sample dilution and sample preparation process for detection. Note that the detection assay considers the dilution of the spiked cortisol. Table 1 summarizes that the recovery rates of the detection are 95.00 and 107.24%.

Table 1. Spike Recovery Rate of Cortisol Detection in Saliva Samples (n = 3)

spiked cortisol concentration (nM)	cortisol conc. after sample dilution (nM)	detected concentration (nM)	mean recovery rate (%)
12.5	2.5	$2.37 \pm 0.29$	95.00
125	25	$26.81 \pm 4.81$	107.24

#### CONCLUSIONS

We explored the fluorescence quenching of QDs induced by multiple types of steroid hormones and further utilized the unique target-induced quenching property to demonstrate a new kind of cortisol sensor. The sensor relies on the modulation of QD quenching efficiency in response to the change in the cortisol concentration. Both the cortisol-selective aptamers and anticortisol antibodies grafted on QDs rendered the selectivity of the nanosensors. The aptamer-based nanosensors offered a higher quenching efficiency and yielded a detection limit of about 1 nM and a broader linear detection range (0.4–400 nM). In contrast, the antibody-based nano-

sensors provided a detection limit of about 100 pM, probably due to the lower dissociation constant. The label-free detection does not require an additional labeling process leading to a short detection time of 20 min. The simplified cortisol detection was successfully demonstrated using saliva samples. The sample dilution and sample preparation process were optimized to achieve sensitive, consistent detection. The results suggest that the target-induced quenching holds great promise in the analysis of cortisol and could be extended to detect other steroid hormones. The facile, sensitive detection method is expected to provide an alternative approach to the point-of-care analysis of steroid hormones.

#### ASSOCIATED CONTENT

### Supporting Information

The Supporting Information is available free of charge at https://pubs.acs.org/doi/10.1021/acs.langmuir.0c00513.

Experimental results regarding the effect of quantum dot types, buffer ionic strength, and sample preparation methods on sensing performance (PDF)

# AUTHOR INFORMATION

# **Corresponding Author**

Li-Jing Cheng — Electrical Engineering and Computer Science, Oregon State University, Corvallis, Oregon 97331, United States; ⊙ orcid.org/0000-0002-1386-9368; Email: chengli@ oregonstate.edu

### **Authors**

Ye Liu — Electrical Engineering and Computer Science, Oregon State University, Corvallis, Oregon 97331, United States

**Bo Wu** – Electrical Engineering and Computer Science, Oregon State University, Corvallis, Oregon 97331, United States

Ekembu K. Tanyi — Electrical Engineering and Computer Science, Oregon State University, Corvallis, Oregon 97331, United States

Sanjida Yeasmin — Electrical Engineering and Computer Science, Oregon State University, Corvallis, Oregon 97331, United States

Complete contact information is available at: https://pubs.acs.org/10.1021/acs.langmuir.0c00513

#### **Notes**

The authors declare no competing financial interest.

#### ACKNOWLEDGMENTS

The authors acknowledge partial financial support from the National Science Foundation (nos. 1810067 and 1512816) and National Institutes of Health (no. 1R21DE027170-01).

#### REFERENCES

- (1) Kirschbaum, C.; Wolf, O. T.; May, M.; Wippich, W.; Hellhammer, D. H. Stress- and treatment-induced elevations of cortisol levels associated with impaired declarative memory in healthy adults. *Life Sci.* **1996**, *58*, 1475–1483.
- (2) Laudat, M.; Cerdas, S.; Fournier, C.; Guiban, D.; Guilhaume, B.; Luton, J. Salivary cortisol measurement: a practical approach to assess pituitary-adrenal function. *J. Clin. Endocrinol. Metab.* **1988**, *66*, 343–348.
- (3) Papanicolaou, D. A.; Mullen, N.; Kyrou, I.; Nieman, L. K. Nighttime salivary cortisol: a useful test for the diagnosis of Cushing's syndrome. *J. Clin. Endocrinol. Metab.* **2002**, *87*, 4515–4521.
- (4) Sturmer, L. R.; Dodd, D.; Chao, C. S.; Shi, R.-Z. Clinical utility of an ultrasensitive late night salivary cortisol assay by tandem mass spectrometry. *Steroids* **2018**, *129*, 35–40.
- (5) Nieman, L. K.; Biller, B. M.; Findling, J. W.; Newell-Price, J.; Savage, M. O.; Stewart, P. M.; Montori, V. M. The diagnosis of Cushing's syndrome: an endocrine society clinical practice guideline. *J. Clin. Endocrinol. Metab.* **2008**, 93, 1526–1540.
- (6) Vogeser, M.; Durner, J.; Seliger, E.; Auernhammer, C. Measurement of late-night salivary cortisol with an automated immunoassay system. *Clin. Chem. Lab. Med.* **2006**, *44*, 1441–1445.
- (7) Lewis, J.; Elder, P. An enzyme-linked immunosorbent assay (ELISA) for plasma cortisol. *J. Steroid Biochem. Mol. Biol.* **1985**, 22, 673–676.
- (8) Lewis, J. G.; Manley, L.; Whitlow, J. C.; Elder, P. A. Production of a monoclonal antibody to cortisol: application to a direct enzymelinked immunosorbent assay of plasma. *Steroids* **1992**, *57*, 82–85.
- (9) Yeh, C.-M.; Glöck, M.; Ryu, S. An optimized whole-body cortisol quantification method for assessing stress levels in larval zebrafish. *PLoS One* **2013**, *8*, No. e79406.
- (10) Tiller, K. E.; Tessier, P. M. Advances in antibody design. *Annu. Rev. Biomed. Eng.* **2015**, *17*, 191–216.
- (11) Teicher, B. A.; Chari, R. V. Antibody conjugate therapeutics: challenges and potential. *Clin. Cancer Res.* **2011**, *17*, 6389–6397.
- (12) Kim, J.; Valdés-Ramírez, G.; Bandodkar, A. J.; Jia, W.; Martinez, A. G.; Ramírez, J.; Mercier, P.; Wang, J. Non-invasive mouthguard biosensor for continuous salivary monitoring of metabolites. *Analyst* **2014**, *139*, 1632–1636.
- (13) Fu, H.-J.; Yuan, L.-P.; Shen, Y.-D.; Liu, Y.-X.; Liu, B.; Zhang, S.-W.; Xie, Z.-X.; Lei, H.-T.; Sun, Y.-M.; Xu, Z.-L. A full-automated magnetic particle-based chemiluminescence immunoassay for rapid detection of cortisol in milk. *Anal. Chim. Acta* **2018**, *1035*, 129–135.
- (14) Zainol Abidin, A. S.; Rahim, R.; Md Arshad, M.; Fatin Nabilah, M.; Voon, C.; Tang, T.-H.; Citartan, M. Current and potential developments of cortisol aptasensing towards point-of-care diagnostics (POTC). Sensors 2017, 17, No. 1180.
- (15) Pfeiffer, F.; Mayer, G. Selection and biosensor application of aptamers for small molecules. *Front. Chem.* **2016**, *4*, No. 25.
- (16) Lakhin, A.; Tarantul, V.; Gening, L. Aptamers: problems, solutions and prospects. *Acta Nat.* **2013**, *5*, 34–43.
- (17) Song, S.; Wang, L.; Li, J.; Fan, C.; Zhao, J. Aptamer-based biosensors. *TrAC*, *Trends Anal. Chem.* **2008**, *27*, 108–117.
- (18) Tombelli, S.; Minunni, M.; Mascini, M. Analytical applications of aptamers. *Biosens. Bioelectron.* **2005**, 20, 2424–2434.
- (19) Zhou, W.; Huang, P.-J. J.; Ding, J.; Liu, J. Aptamer-based biosensors for biomedical diagnostics. *Analyst* **2014**, *139*, 2627–2640.
- (20) Li, J. J.; Fang, X.; Tan, W. Molecular aptamer beacons for real-time protein recognition. *Biochem. Biophys. Res. Commun.* **2002**, 292, 31–40
- (21) Mitchell, J. S.; Lowe, T. E.; Ingram, J. R. Rapid ultrasensitive measurement of salivary cortisol using nano-linker chemistry coupled

- with surface plasmon resonance detection. *Analyst* **2009**, *134*, 380–386.
- (22) Jo, S.; Lee, W.; Park, J.; Kim, W.; Kim, W.; Lee, G.; Lee, H.-J.; Hong, J.; Park, J. Localized surface plasmon resonance aptasensor for the highly sensitive direct detection of cortisol in human saliva. *Sens. Actuators, B* **2020**, 304, No. 127424.
- (23) Tlili, C.; Myung, N. V.; Shetty, V.; Mulchandani, A. Label-free, chemiresistor immunosensor for stress biomarker cortisol in saliva. *Biosens. Bioelectron.* **2011**, *26*, 4382–4386.
- (24) Dhull, N.; Kaur, G.; Gupta, V.; Tomar, M. Highly sensitive and non-invasive electrochemical immunosensor for salivary cortisol detection. *Sens. Actuators, B* **2019**, 293, 281–288.
- (25) Spano, G.; Cavalera, S.; Di Nardo, F.; Giovannoli, C.; Anfossi, L.; Baggiani, C. Development of a biomimetic enzyme-linked immunosorbent assay based on a molecularly imprinted polymer for the detection of cortisol in human saliva. *Anal. Methods* **2019**, *11*, 2320–2326
- (26) Liu, Y.; Kannegulla, A.; Wu, B.; Cheng, L.-J. Quantum dot fullerene-based molecular beacon nanosensors for rapid, highly sensitive nucleic acid detection. *ACS Appl. Mater. Interfaces* **2018**, 10, 18524–18531.
- (27) Resch-Genger, U.; Grabolle, M.; Cavaliere-Jaricot, S.; Nitschke, R.; Nann, T. Quantum dots versus organic dyes as fluorescent labels. *Nat. Methods* **2008**, *5*, 763–775.
- (28) Smith, A. M.; Nie, S. Semiconductor nanocrystals: structure, properties, and band gap engineering. *Acc. Chem. Res.* **2010**, *43*, 190–200.
- (29) Attia, M. S.; El-Swafy, E.; Youssef, A. O.; Hefny, H.; Khalil, M. A Novel Method for the Assessment of Cortisol Hormone in Different Body Fluids Using A New Photo Probe Thiazole Derivative. *J. Fluoresc.* **2014**, *24*, 337–344.
- (30) Szent-Györgyi, A. Charge transfer and electronic mobility. *Proc. Natl. Acad. Sci. U.S.A.* **1967**, *58*, 2012–2014.
- (31) Allison, A. C.; Peover, M.; Gough, T. Electron donor and acceptor capacity of some hormones. *Life Sci.* **1962**, *1*, 729–737.
- (32) Siegberg, D.; Herten, D.-P. Fluorescence Quenching of Quantum Dots by DNA Nucleotides and Amino Acids1. *Aust. J. Chem.* **2011**, *64*, 512–516.
- (33) Bruno, J. G.; Carrillo, M. P.; Phillips, T.; Hanson, D.; Bohmann, J. A. DNA aptamer beacon assay for C-telopeptide and handheld fluorometer to monitor bone resorption. *J. Fluoresc.* **2011**, *21*, 2021–2033.
- (34) Rao, A. N.; Grainger, D. W. Biophysical properties of nucleic acids at surfaces relevant to microarray performance. *Biomater. Sci.* **2014**, 2, 436–471.
- (35) Saha, B.; Evers, T. H.; Prins, M. W. How antibody surface coverage on nanoparticles determines the activity and kinetics of antigen capturing for biosensing. *Anal. Chem.* **2014**, *86*, 8158–8166.